

Ab initio calculation of second-harmonic-generation at the Si(100) surface

Bernardo S. Mendoza*

Centro de Investigaciones en Optica, A. C., León, Guanajuato, México

Maurizia Palumbo, Giovanni Onida, and Rodolfo Del Sole

Istituto Nazionale per la Fisica della Materia-Dipartimento di Fisica, II Università di Roma Tor Vergata, Rome, Italy

(Received 16 January 2001; published 18 April 2001)

We present a microscopic, first-principles calculation of the second-harmonic spectra of clean and Hydrogenated Si(100) surfaces. The differences between theoretical spectra obtained for different reconstructions, namely the 2×1 and the $c(4\times 2)$ ones, are dramatically enhanced with respect to those obtained in linear optical response. The calculated spectral features are analyzed in detail, studying their relations with those of bulk and surface linear optical spectra. The inclusion of quasiparticle effects within the scissors operator approximation yields theoretical spectra in good agreement with the experiments.

DOI: 10.1103/PhysRevB.63.205406

PACS number(s): 78.66.-w, 42.65.An, 42.65.Ky

I. INTRODUCTION

As experimental nonlinear optical techniques become more widely used in surface physics studies, more refined and precise methods of theoretical calculation are needed to render this kind of spectroscopies physically sound. In particular, second-harmonic generation (SHG) at centrosymmetric-semiconductor surfaces has been used with great success to investigate experimentally a wide range of surface related phenomena.¹⁻⁴ The surface sensitivity stems from the fact that, within the dipole approximation, SHG is forbidden inside the bulk of centrosymmetric crystals. However, at the surface, where inversion symmetry is broken, dipolar SHG is allowed. On the theoretical side, some of us recently reported a successful calculation of SHG from clean and H-covered Si(100) surfaces.⁵ The calculation of the nonlinear surface susceptibility tensor $\tilde{\chi}$ was carried out according to the semiempirical tight-binding (SETB) method, where the equilibrium atomic positions for the different surfaces were obtained through the density-functional theory within the local-density approximation (DFT-LDA). Atomic positions calculated in this way are usually accurate within less than a tenth of an Angstrom.

This scheme has been frequently and successfully employed to study also the linear optical properties of semiconductor surfaces.^{6,7} However, its semiempirical character, the lack of self-consistency, the limited basis set, and other approximations usually employed make it not completely satisfactory. For this reason, *ab initio* approaches, where the electronic structure is consistently calculated within DFT-LDA, or including self-energy effects according to Green's-function theory (where the resulting energy levels are accurate within 0.1 eV), or even including the electron-hole interaction, have been recently applied to study the linear optical properties of semiconductor surfaces.⁸⁻¹⁰ While qualitative agreement is generally obtained with SETB results, important discrepancies occur in some cases, for instance in the reflectance anisotropy of Si(100).⁸

In this paper we apply the *ab initio* approach, used in the case of linear optical properties, to calculate the SHG at semiconductor surfaces. We use Si(100) as a test case. The

purpose of the paper is to assess: (i) the effect of quasiparticle (QP) corrections on SHG spectra; and (ii) their sensitivity to the atomic structure of the surface.

Ab initio calculations have been recently carried out by Gavrilenko *et al.*¹¹ for the clean 2×1 , H-covered monohydride, and Ge-covered Si(100) surfaces, and by Lim *et al.*¹² for the boron-covered surface, without including QP corrections. Here, we consider the most stable $c(4\times 2)$ reconstruction of the clean surface, and a number of different H-covered phases. We find nontrivial QP effects and important differences between the spectra calculated for the $c(4\times 2)$ and 2×1 reconstructions, the former being in better agreement with experimental data.

The paper is organized as follows. In Sec. II we give the basic formulas needed to calculate the SHG radiated efficiency. In Sec. III we present and discuss the results and in Sec. IV we give the conclusion.

II. THEORY

We calculate the reflected SHG efficiency \mathcal{R} through the second-order surface susceptibility tensor $\tilde{\chi}$. For an isotropic surface, such as the double-domain Si(100) surface considered here, the p -polarized SH output is given by

$$\mathcal{R}_{pi} = \frac{32\pi^3}{(n_0e)^2c^3} \omega^2 \tan^2\theta |T_p(2\omega)T_i^2(\omega)r_{pi}|^2, \quad (1)$$

where $i=s$ or p indicates the polarization of the incoming photon of frequency ω . Here,

$$r_{pp} = \sin^2\theta \chi_{\perp\perp\perp} + (c/\omega)^2 k_{\perp}^2(\omega) \chi_{\perp\parallel\parallel} - (c/\omega)^2 k_{\perp}(\omega) k_{\perp}(2\omega) \chi_{\parallel\perp\perp}, \quad (2)$$

and $r_{ps} = \chi_{\perp\parallel\parallel}$. The s -polarized SH is identically zero due to symmetry considerations. In the equations above, θ is the angle of incidence, c the speed of light, e the electron charge, n_0 the electron density of the system, T_i the transmission Fresnel factor for the i polarization, and $k_{\perp} = (\omega/c)[\epsilon(\omega) - \sin^2\theta]^{1/2}$, $\epsilon(\omega)$ being the bulk dielectric function. We notice that all components of $\tilde{\chi}$ different from zero contribute

to \mathcal{R}_{pp} . These expressions are strictly valid within the dipole approximation. Nevertheless, even if quadrupolar corrections are considered, the isotropic and anisotropic bulk quadrupole terms in \mathcal{R} ,¹³ have been shown to yield negligible contributions as compared to the surface dipole terms.^{14–16}

The key ingredient of the calculation is $\vec{\chi}$ for the double-domain surface considered here. Following Ref. 17, we briefly sketch the procedure taken to calculate it. We model the semi-infinite crystal by a slab of N atomic planes. The imaginary part of the single-domain second-order surface susceptibility \vec{X} is given by

$$\begin{aligned} \Im m[X_{ijk}(\omega)] &= \frac{\pi n_0 e^4}{2 A m^3 \omega^3} \sum_{\vec{k}} \sum_{r \in C} \sum_{s \in V} \left\{ \sum_{n \in C} \left[\left(\frac{\mathcal{P}_{sn}^i \mathcal{P}_{nr}^j \mathcal{P}_{rs}^k}{E_{ns} - 2E_{rs}} \right. \right. \right. \\ &+ \left. \left. \frac{\mathcal{P}_{sn}^j \mathcal{P}_{nr}^i \mathcal{P}_{rs}^k}{E_{ns} + E_{rs}} \right) \delta(E_{rs} - \hbar\omega) \right. \\ &- \left. \left. 2 \frac{\mathcal{P}_{sn}^i \mathcal{P}_{nr}^j \mathcal{P}_{rs}^k}{E_{ns} - 2E_{rs}} \delta(E_{ns} - 2\hbar\omega) \right] \right. \\ &- \sum_{m \in V} \left[\left(\frac{\mathcal{P}_{mr}^i \mathcal{P}_{sm}^j \mathcal{P}_{rs}^k}{E_{rm} - 2E_{rs}} + \frac{\mathcal{P}_{mr}^j \mathcal{P}_{sm}^i \mathcal{P}_{rs}^k}{E_{rm} + E_{rs}} \right) \delta(E_{rs} - \hbar\omega) \right. \\ &- \left. \left. 2 \frac{\mathcal{P}_{mr}^i \mathcal{P}_{sm}^j \mathcal{P}_{rs}^k}{E_{rm} - 2E_{rs}} \delta(E_{rm} - 2\hbar\omega) \right) \right] \left. \right\}, \quad (3) \end{aligned}$$

where $P_{s,n}^i(\vec{k})$ is the matrix element of the i -Cartesian component of the momentum operator (\vec{P}) between states s and n , which may be valence (V), or conduction (C) states at point \vec{k} in the two-dimensional Brillouin zone, A is the sample area, $E_{nr} = E_n(\vec{k}) - E_r(\vec{k})$, $E_n(\vec{k})$ being the one-electron energy. We remark that the above expressions must be symmetrized in the last two indices (jk) in order to comply with the intrinsic permutation symmetry of X , and employ the Kramers-Kronig transform to calculate the real part of \vec{X} . Then, the components of $\vec{\chi}$ for the double-domain (100) surface are obtained through

$$\chi_{\perp\perp\perp} = X_{zzz}, \quad (4a)$$

$$\chi_{\perp\parallel\parallel} = (X_{zxx} + X_{zyy})/2, \quad (4b)$$

$$\chi_{\parallel\parallel\perp} = (X_{xxz} + X_{yyz})/2, \quad (4c)$$

where $X_{ijk} = X_{ikj}$ are calculated for each of the two single-domain lattices. Notice that $X_{zxx}^I = X_{zyy}^{II}$, and $X_{xxz}^I = X_{yyz}^{II}$, for domain I and domain II.

In the calculation of X_{ijk} , the fundamental electric field oscillating at ω that induces the nonlinear response, is taken inside the surface. In particular, these fields are simply given by the external fields properly multiplied by the corresponding Fresnel factors.¹⁷ A more detailed description of the fields, which incorporates the spatial variation of the dielectric function near the surface within the three-layer model,¹⁷ shows no change in the SHG peaks positions, and only a

slight difference in their intensity. However, the full treatment of the surface screening is still lacking, and further improvement of the present formulation can be made along this point. This screening will presumably affect more the zzz component of \vec{X} than any other component, however, it is not at all trivial to anticipate what the actual effect will be, and thus, we explain the results within our approximation. Also, excitonic and local-field effects have been included so far only in the case of *simple* surfaces, as Si(111)2 \times 1.¹⁰ This surface is *simple* in the sense that its optical properties in the lowest-energy range (below 1 eV) can be calculated by considering only one filled and one empty surface band, in a limited k -space region where they have a small dispersion. This of course greatly reduces the number of electron-hole states used to build up the excitons and makes the excitonic calculation feasible. This is not the case of Si(100), where a lot of bulk states must be considered, for energetic reasons, together with surface states. Therefore, at the present stage of the available calculations for optical properties of semiconducting surfaces, like the one presented here, local-field and excitonic effects are still beyond current capabilities for Si(100)2 \times 1 and $c(4\times 2)$ and are thus neglected throughout.

The fact that we use a repeated slab in order to model the semi-infinite crystal brings about the complication that such a system is intrinsically centrosymmetric. Therefore, in order to describe the emission of SH light, we introduce the modified momentum operator $\vec{P} = [S(z)\vec{P} + \vec{P}S(z)]/2$, where $\vec{P} = -i\hbar\vec{\nabla}$ is the usual momentum operator, and $S(z)$ is a function of z , being 1 at the front surface and 0 at the back surface. This function allows us to avoid the spurious destructive interference of SH light generated at the two surfaces of the slab. However, the calculation of the \vec{P} matrix elements is computationally heavier than that of \vec{P} matrix elements in a plane-wave basis, since \vec{P} is diagonal therein, while \vec{P} is not. To overcome this problem, the matrix elements of \vec{P} , required in Eq. (3), are calculated according to

$$\vec{P}_{mn} = \frac{1}{2} \sum_s (S_{ms}\vec{P}_{sn} + \vec{P}_{ms}S_{sn}), \quad (5)$$

where the completeness relation for the states of the slab has been used. Expanding the wave functions as $\psi_{n\vec{k}}(\vec{r}) = \sum_{\vec{G}} c_{n\vec{G}}(\vec{k}) \exp[i(\vec{k} + \vec{G}) \cdot \vec{r}]$ (where all plane waves up to a cutoff of 15 Rydberg are included), it is straightforward to obtain that

$$S_{mn} = \sum_{\vec{G}\vec{G}'} c_{m\vec{G}'}^*(\vec{k}) c_{n\vec{G}}(\vec{k}) \delta_{\vec{G}\vec{G}'} f(g - g'), \quad (6)$$

with

$$f(g) = \int_0^d dz S(z) e^{-igz}. \quad (7)$$

Here, $\vec{G} = \vec{G}_{\parallel} + g\hat{z}$, are the vectors of the reciprocal lattice, and d is the slab periodicity. For $S(z)$ we have used a step function centered at the middle of the slab. Using smoother

functions yields the same SHG line shape with only small changes in the absolute magnitude of \mathcal{R} .¹⁷

The *ab initio* DFT-LDA calculation of the optical properties of solids, produces gaps that are smaller than the experimental ones by about 0.5–1 eV in semiconductors, leading to redshifted spectra.¹⁸ In principle, one should go into a many-body formalism to improve beyond DFT-LDA.^{10,19–22} In practice one has to consider an effective single-QP Hamiltonian, where self-energy effects are described according to Hedin’s GW approximation²³ and the electron-hole interaction is neglected. The effect of the QP corrections on the linear optical spectra of semiconductors can be calculated by assuming nearly identical DFT-LDA and QP wave functions, and by following the next two steps due to Del Sole and Girlanda:²⁴ first, the LDA energies $E_n(\vec{k})$ are shifted by $\Delta_n(\vec{k})$, and second, the momentum matrix elements \vec{P}_{mn} are renormalized according to

$$\vec{P}_{mn}^{\text{eff}} = \vec{P}_{mn} \frac{E_m(\vec{k}) + \Delta_m(\vec{k}) - E_n(\vec{k}) - \Delta_n(\vec{k})}{E_m(\vec{k}) - E_n(\vec{k})}. \quad (8)$$

We use the scissors-operator approximation, used in Ref. 25, for the calculation of the linear optical response (bulk) of Si and Ge, in which the conduction bands are rigidly upward shifted by a constant $\Delta_n(\vec{k}) = \Delta$ with respect to the valence bands. In Eq. (3) we replace $E_n(\vec{k}) \rightarrow E_n(\vec{k}) + \Delta$ if n is a conduction (C) state, and replace the C-valence(V) matrix elements of \vec{P} , by

$$\vec{P}_{CV}^{\text{eff}} = \vec{P}_{CV} \frac{E_C(\vec{k}) - E_V(\vec{k}) + \Delta}{E_C(\vec{k}) - E_V(\vec{k})}. \quad (9)$$

This renormalization stems from the nonlocal character of the self-energy. If the scissors-operator approximation is used naively, that is without renormalizing the optical matrix elements according to Eq. (9), spectral intensities and dielectric constants are underestimated by about 30 percent in Si.²⁵ This procedure has been recently applied also to the calculation of bulk SHG spectra in III-IV compounds.²⁶

At present, the QP calculation outlined above is the best that can be done for this surface, which, on the other hand, has become prototypical for SHG experiment and theory. We mention, though, that excitonic and local-field effects, along with the surface screening, might be crucial for a quantitative comparison between theory and experiment.

III. RESULTS

Energy minimization reveals that the most favorable structure for the clean Si(100) surface corresponds to a $c(4 \times 2)$ reconstruction, where the Si-Si dimers alternate in buckling from one neighbor to another in the surface plane.²⁷ Although reflection high-energy electron diffraction (RHEED) shows a 2×1 unit cell at room temperature, the local structure is expected to be $c(4 \times 2)$.²⁷ In Fig. 1 we show the p -in p -out SHG efficiency, \mathcal{R}_{pp} , of the $c(4 \times 2)$ reconstructed clean Si(100) surface, where the broadening for the Kramers-Kronig transform is set to 25 meV. We re-

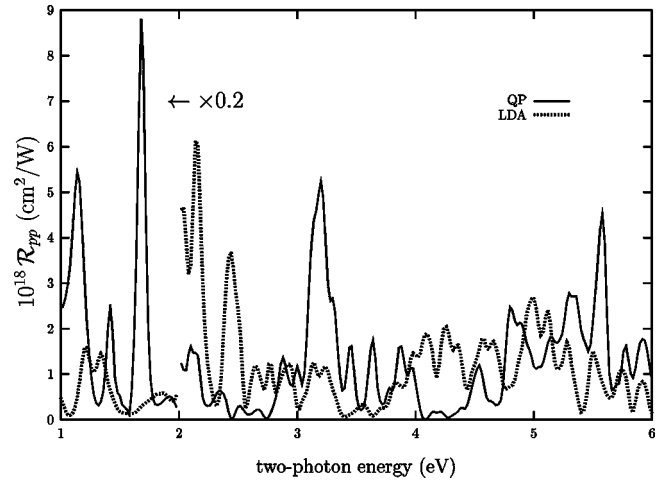


FIG. 1. We show \mathcal{R}_{pp} vs the two-photon energy for the $c(4 \times 2)$ Si(100) surface. The angle of incidence $\theta = 55^\circ$ is the same as in the experiment of Ref. 4, and a broadening of 25 meV is used. The solid line corresponds to $\Delta = 0.5$ eV, that is with QP corrections, whereas the dotted line is for $\Delta = 0$, corresponding to the LDA result.

port both the $\Delta = 0$ result (i.e., the bare LDA), and the $\Delta = 0.5$ eV result (i.e., including QP corrections within the scissors-operator approximation).²⁸ We notice that QP corrections not only shift the resonances to higher energies, but also substantially redistribute their weights, as a consequence of the different shifts of 1ω and 2ω resonances in Eq. (3). For the spectrum with $\Delta = 0.5$ eV, the E_1 peak is clearly seen at 3.2 eV, E_2 is seen just above 4.5 eV, and the E'_1 bulk transition is present at 5.3 eV. We also notice several peaks below E_1 , which come from transitions involving dangling-bondlike surface states.⁵ An important observation from the spectra is that several bulk interband transitions known from linear optics, such as E'_1 , are present and, in contrast with the linear case, show a comparable magnitude with respect to E_1 and E_2 .

We have carefully checked the convergence of the calculation with respect to the number of k points used to calculate the susceptibility, to the number of layers in the slab, and to the thickness of the vacuum layer between the slabs, using the 2×1 reconstruction as the test case. We found that good convergence is achieved using 256 k points in the irreducible rectangle of the surface Brillouin zone (SBZ), and four empty atomic layers between the slabs. In Fig. 2 we show \mathcal{R}_{pp} for a 2×1 reconstructed clean Si(100) surface, with $\Delta = 0.5$ eV for various slab thicknesses, where the broadening for the Kramers-Kronig transform is set to 50 meV. We see that the curves for 16 and 20 layers are similar to each other, although markedly different from that with 12 layers. Hence, we assume that 16 layers are enough to ensure good convergence, and use the same thickness for all the reconstructions studied here. In the case of $c(4 \times 2)$, we checked that 32 or 64 special k points in the irreducible SBZ yield similar results. The converged spectra for the 2×1 reconstruction, shown in Fig. 2 (16 and 20 layers), are significantly different from that of the $c(4 \times 2)$ surface shown in Fig. 1, and their overall intensities are about *seven times* smaller. The 20-

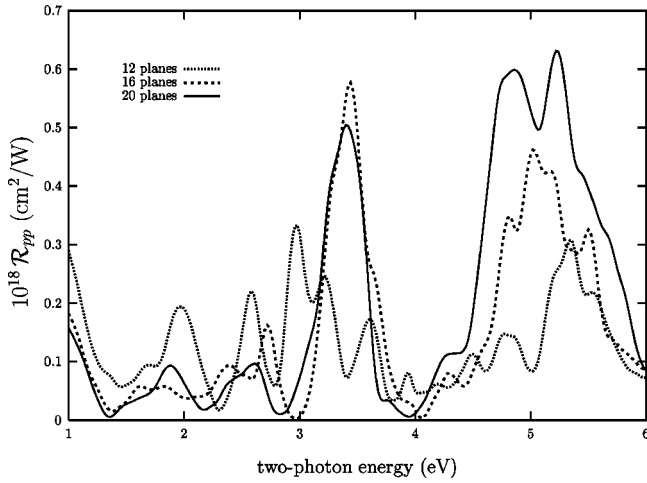


FIG. 2. Same as Fig. 1, but for a 2×1 reconstruction of the clean Si(100) surface for 12 (dotted), 16 (dashed), and 20 (solid) planes. The broadening in this case is 50 meV.

layers spectrum has peaks or shoulders at 1.5, 1.9, 2.4, and 2.6 eV, that are due to 2ω surface-state resonances, appearing also in the reflectance anisotropy (RAS) and/or surface differential reflectivity (SDR) spectra of Ref. 8 at nearby frequencies. 1ω resonances corresponding to the second, third, and fourth structure mentioned above appear at about 3.8, 4.8, and 5.2 eV (of course, a 1ω resonance occurs at a frequency that is twice that of the corresponding 2ω resonance); the latter two merge with the 2ω resonance corresponding to E_2 , around 4.6 eV, and that corresponding to E'_1 around 5 eV. The strong peak at 3.3 eV is the 2ω resonance corresponding to E_1 . Our converged spectra for 16 and 20 layers are similar to that of Gavrilenko *et al.*,¹¹ in the energy range where they show experimental data (around 3.3 eV), although there is a slab of only 12 layers and a different theoretical framework was used, suggesting that subtle error cancellations may occur in SH calculations.

The comparison with experiment is qualitatively good for the QP-corrected SHG spectrum obtained for the $c(4 \times 2)$ reconstruction. As it is shown in Fig. 3, the low-temperature experimental spectrum has, besides the E_1 peak at 3.4 eV, a peak at 3.0 eV,⁴ which is reproduced by the calculation and mainly explained in terms of a 1ω -resonant transition across surface states.³² We notice that the calculated spectrum is redshifted with respect to the experiment by about 0.2 eV. For comparison, the spectrum for the 2×1 surface is also shown with a much weaker intensity (multiplied by seven in order to be seen in the plot). The finer detail of this spectrum as compared with that of Fig. 2 is due to the smaller broadening of 25 meV used in Fig. 3. Although this spectrum has a different line shape as that of the $c(4 \times 2)$, as we mention before, it also has the E_1 peak at 3.2 eV, and the surface-related peak at 2.8 eV, which is 0.1 eV below the corresponding peak of the $c(4 \times 2)$. As seen from Fig. 3, the ratio of the intensity of the surface peak and E_1 peak, and the energy separation is in better agreement with that of the experiment for the $c(4 \times 2)$ than for the 2×1 surface reconstruction. We also notice that both surfaces present a small peak in between the last two peaks that is not resolved in the

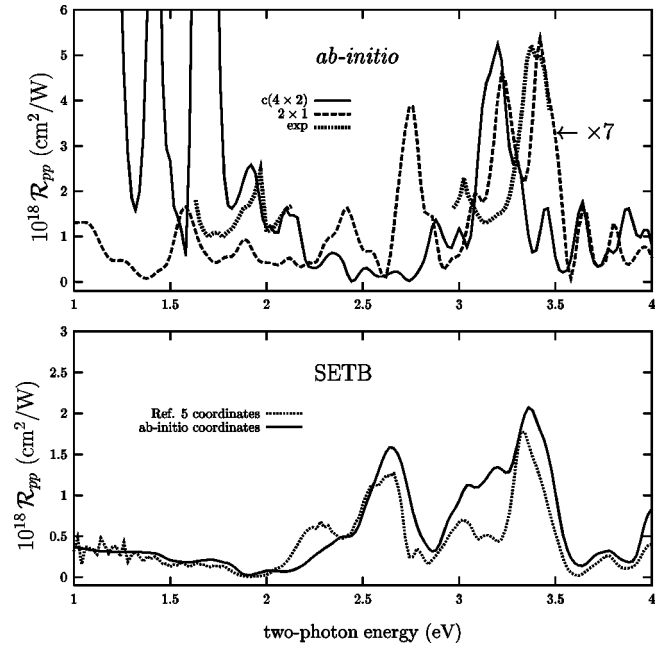


FIG. 3. Same as Fig. 1. The top panel shows the $c(4 \times 2)$ (solid line) and the 2×1 (dashed line, multiplied by 7) spectra for $\Delta = 0.5$ eV. The dotted lines show the low-temperature experimental results of Ref. 4 (around E_1) and of Ref. 29 (around 2 eV), both rescaled on the vertical axis. The bottom panel shows the SETB spectra, where the solid line is for the same coordinates as the solid line of the top panel, and the dotted line is for the coordinates of Ref. 5 (see text for details).

experiment. We have also plotted some newly obtained SHG data around 2 eV,²⁹ where we see that there is also a nice agreement with the theoretical spectrum of the $c(4 \times 2)$ or the 2×1 surface. We mention that neither experiment gave absolute values for \mathcal{R} , but the low-frequency data showed less counts than the E_1 SHG data.²⁹ In this figure we also show (bottom panel) the spectra for the $c(4 \times 2)$ surface as obtained within the SETB formalism described in Ref. 5, with the same set of coordinates as in this reference, and the set of coordinates calculated in Ref. 8 and used here. The two SETB spectra are rather similar to each other. The comparison with the *ab initio* spectrum above 2 eV is satisfactory, although important differences are present below this energy. They are related to the wrong sign predicted by SETB in the linear optical technique of reflectance anisotropy in this energy range.⁸

As we mentioned before, within the dipole approximation the s -polarized SH output is identically zero due to symmetry. However, the p -polarized SH is also possible for an s -polarized beam. Indeed, as given above, $r_{ps} = \chi_{\perp \parallel}$, thus, \mathcal{R}_{ps} only samples one component of $\tilde{\chi}$. Although, no experimental spectrum has been reported for this combination of polarization on Si(100), we show in Fig. 4 \mathcal{R}_{ps} for the $c(4 \times 2)$ and 2×1 surface reconstructions. We notice that both spectra show well-defined E_1 peak (around 3.3 eV) and surface peaks, and the bulk peaks are also present, although not as well defined as for the \mathcal{R}_{pp} case. Also, the intensity of the 2×1 is much smaller than for that of the $c(4 \times 2)$ case, especially below 2.5 eV. Finally, we mention that the overall intensity of \mathcal{R}_{ps} is at least an order of magnitude smaller

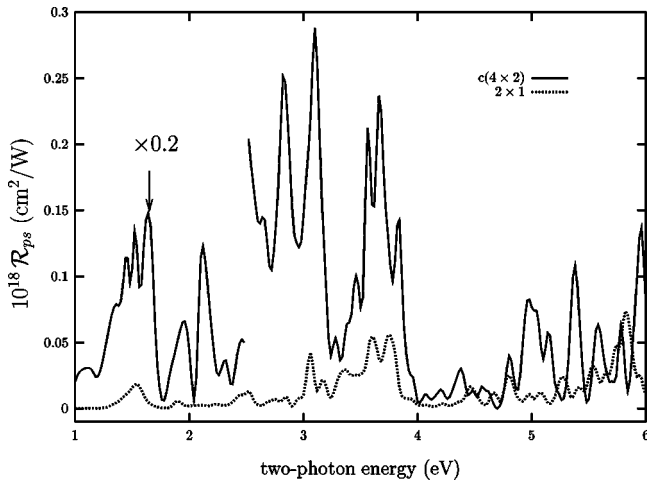


FIG. 4. We show \mathcal{R}_{ps} vs the two-photon energy for the $c(4 \times 2)$ (solid line) and the 2×1 (dotted line) Si(100) surface. \mathcal{R}_{ps} gives the p -polarized SH efficiency for a s -polarized input beam. The angle of incidence is $\theta = 55^\circ$ and a broadening of 25 meV is used. Both cases are for QP corrections with $\Delta = 0.5$ eV.

than that of \mathcal{R}_{pp} , a fact that might explain the lack of measurements for this much weaker SH signal.

To complete this paper, in Fig. 5 we show \mathcal{R}_{pp} for a 2×1 reconstructed H-covered Si(100) surface, including QP corrections with $\Delta = 0.5$ eV. We show spectra for one H per surface dimer, for 2 H per surface dimer (which corresponds to the monohydride phase), and for the ideally terminated surface, where the dimer is broken due to the bonding of 2H per surface Si. We mention that at the monohydride and dihydride surface, there are no surface states in the near-gap region, while some of them survive at the partially saturated surface with one H per dimer. We see that complete H saturation quenches all structures below 3.5 eV, which are due to transitions involving surface states. The comparison with the

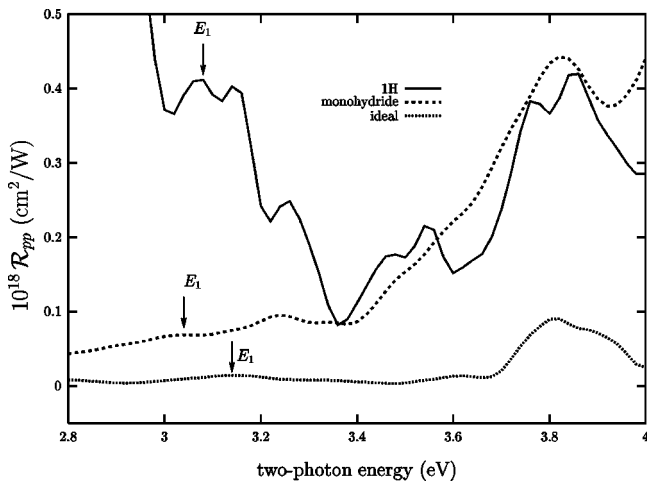


FIG. 5. Same as Fig. 1, but for H covered 2×1 reconstructions of the Si(100) surface. The solid line is for one H per surface dimer, the dashed line is for the monohydride phase, and the dotted line is for the ideally terminated surface (4 H per dimer). The vertical arrows denote the positions of E_1 .

unshifted spectra (i.e., those with $\Delta = 0$, not shown here) reveals that, different from the case of the clean surface, shifted and unshifted spectra are similar to each other, apart from the shift. This is obviously due to the lack of the interference of the 1ω surface-state resonances with the 2ω E_1 and E_2 resonances. We notice that the E_1 peak is shifted from its position at 3.2 eV in the clean $c(4 \times 2)$ surface (see Fig. 1), to about 3.08 eV for the one H per dimer surface, and to 3.04 eV for the monohydride surface. For the ideal surface (4 H per dimer), E_1 is at 3.14 eV. Also, the intensity of the E_1 peak is strongly reduced as compared with the clean surface. The redshifted spectra and the quenching of the E_1 peak as a consequence of H absorption are in qualitative agreement with experiment.⁴ Moreover, as we move from the monohydride to the ideally terminated surface, the blue-shifted E_1 peak is also observed experimentally.⁴ These shifts are obtained within SETB only by assuming the presence of suitable built-in near-surface electric fields.³⁰

IV. CONCLUSION

Comparing the SHG experimental findings for this surface with the theoretical spectra calculated within LDA with QP corrections or within SETB, we may conclude that qualitatively both approaches give the same answer, to wit, that the bulk E_1 resonance occurs in surface SHG spectra through electronic transitions across surface-perturbed bulk states, and that the spectral structures below E_1 are due to transitions across surface states. Also, we find that the $\chi_{\parallel\parallel\perp}$ component of the second-order surface susceptibility is mostly responsible for the observed features. Therefore, it is the interplay of both in-plane and perpendicular components of $\vec{\chi}$ that gives rise to the SH response.⁵ However, important differences between SETB and the present *ab initio* calculation occur below 2 eV (see Fig. 3), which are related to the wrong sign of reflectance anisotropy predicted by SETB in the same energy range.⁸ Moreover, the *ab initio* approach yields overall SHG intensities dramatically dependent on the reconstruction, and shifts of the E_1 peak with H coverage in agreement with experimental findings without any *ad hoc* assumption.

In summary, we have presented an *ab initio* calculation of surface SHG, based on the determination of the equilibrium geometry and of the electron bands within DFT-LDA. When QP effects are included within the scissors-operator approximation, important changes of the spectra occur, due to the interference of 1ω surface-state transitions with 2ω bulk-state transitions, which undergo different shifts. When such interference is absent (as in the case of H-saturated surfaces, where near-gap surface states do not occur), instead, only an almost rigid shift of the spectrum is obtained. This treatment shows good agreement with the experimental spectra of clean and H-covered Si(100) surfaces. We have carefully studied the convergence of the calculated spectra with respect to the number of k points and to the slab thickness. We found that SHG is extremely sensitive to the reconstruction: in particular, $c(4 \times 2)$ and 2×1 reconstructions yield different spectra, the former being about 10 times more intense than the latter. The spectrum of the energetically favorable

$c(4\times 2)$ surface resembles better the experimental one, providing an optical proof of the existence of this specific reconstruction.

ACKNOWLEDGMENTS

We thank L. Mantese and M. C. Downer for allowing us to use their experimental data prior to publication. We thank

partial support of CONACyT-México (26651-E), Italian *Ministero per L'Università e per la Ricerca Scientifica e Tecnologica* (MURST-COFIN99), and by the INFM PRA project *IMESS*. We also acknowledge the allocation of computer resources from INFM Progetto Calcolo Parallelo. We thank S. Goedecker for providing us an efficient code for Fast Fourier Transforms.³¹

*Email: bms@valkirie.cio.mx

- ¹For recent reviews, see M.C. Downer, B.S. Mendoza, and V.I. Gavrilenko, *Surf. Interface Anal.* (to be published); G. Lüpke, *Surf. Sci. Rep.* **35**, 75 (1999); J. McGilp, *Surf. Rev. Lett.* **6**, 529 (1999); Y.R. Shen, *Solid State Commun.* **102**, 221 (1997); Th. Rasing, *J. Magn. Magn. Mater.* **175**, 35 (1997); G. A. Reider and T.F. Heinz, in *Photonic Probes of Surfaces*, edited by P. Halevi (Elsevier, Amsterdam, 1995), p. 413; K. van Hasselt, Ph.D. thesis, University of Nijmegen, The Netherlands, 1997.
- ²W. Daum, H.J. Krause, U. Reichel, and H. Ibach, *Phys. Scr.*, T **49**, 513 (1993); *Phys. Rev. Lett.* **71**, 1234 (1993).
- ³U. Höfer, *Appl. Phys. A: Mater. Sci. Process.* **63**, 533 (1996).
- ⁴J.I. Dadap, X.F. Hu, M.H. Anderson, M.C. Downer, J.K. Lowell, and O.A. Aktsipetrov, *Phys. Rev. B* **56**, 13 367 (1997).
- ⁵B.S. Mendoza, A. Gaggiotti, and R. Del Sole, *Phys. Rev. Lett.* **81**, 3781 (1998).
- ⁶J.R. Power, P. Weightman, S. Bose, A.I. Shkrebti, and R. Del Sole, *Phys. Rev. Lett.* **80**, 3133 (1998); A.I. Shkrebti and R. Del Sole, *ibid.* **70**, 2645 (1993).
- ⁷C. Noguez, C. Beitia, W. Preyss, A.I. Shkrebti, M. Roy, Y. Borensztein, and R. Del Sole, *Phys. Rev. Lett.* **76**, 4923 (1996).
- ⁸M. Palummo, G. Onida, R. Del Sole, and B.S. Mendoza, *Phys. Rev. B* **60**, 2522 (1999).
- ⁹O. Pulci, G. Onida, R. Del Sole, and L. Reining, *Phys. Rev. Lett.* **81**, 5374 (1998).
- ¹⁰M. Rohlfing and S.G. Louie, *Phys. Rev. Lett.* **83**, 856 (1999).
- ¹¹V.I. Gavrilenko, R.Q. Wu, M.C. Downer, J.G. Ekerdt, D. Lim, and P. Parkinson, *Thin Solid Films* **364**, 1 (2000).
- ¹²D. Lim, M.C. Downer, J.G. Ekerdt, N. Arzate, B.S. Mendoza, V.I. Gavrilenko, and R.Q. Wu, *Phys. Rev. Lett.* **84**, 3406 (2000).
- ¹³O.A. Aktsipetrov, I.M. Baranova, and Yu.A. Il'inskii, *Zh. Éksp. Teor. Fiz.* **91**, 287 (1986) [*Sov. Phys. JETP* **64**, 167 (1986)]; J.E. Sipe, D.J. Moss, and H.M. Van Driel, *Phys. Rev. B* **35**, 1129 (1987).
- ¹⁴B.S. Mendoza and W.L. Mochán, *Phys. Rev. B* **53**, R10 473 (1996).
- ¹⁵B.S. Mendoza and W.L. Mochán, *Phys. Rev. B* **55**, 2489 (1997).
- ¹⁶Z. Xu, X.F. Hu, D. Lim, J.G. Ekerdt, and M.C. Downer, *J. Vac. Sci. Technol. B* **15**, 1059 (1997).
- ¹⁷L. Reining, R. Del Sole, M. Cini, and J.G. Ping, *Phys. Rev. B* **50**, 8411 (1994).
- ¹⁸W.E. Pickett, *Comments Solid State Phys.* **12**, 57 (1986).
- ¹⁹G. Onida, L. Reining, R.W. Godby, R. Del Sole, and W. Andreoni, *Phys. Rev. Lett.* **75**, 818 (1995).
- ²⁰M. Rohlfing and S.G. Louie, *Phys. Rev. Lett.* **80**, 3320 (1998).
- ²¹S. Albercht, L. Reining, R. Del Sole, and G. Onida, *Phys. Rev. Lett.* **80**, 4510 (1998).
- ²²L.X. Benedict, E.L. Shirley, and R.B. Bohn, *Phys. Rev. Lett.* **80**, 4514 (1998).
- ²³L. Hedin, *Phys. Rev.* **139**, A796 (1965).
- ²⁴R. Del Sole and R. Girlanda, *Phys. Rev. B* **48**, 11 789 (1993).
- ²⁵Z.H. Levine and D.C. Allan, *Phys. Rev. Lett.* **63**, 1719 (1989).
- ²⁶B. Adolph and F. Bechstedt, *Phys. Rev. B* **57**, 6519 (1998); J.L.P. Hughes and J.E. Sipe, *ibid.* **53**, 10 751 (1996).
- ²⁷A.I. Shkrebti, R. Di Felice, C.M. Bertoni, and R. Del Sole, *Phys. Rev. B* **51**, 11 201 (1995).
- ²⁸ $\Delta=0.5$ eV gives a bulk dielectric function in good agreement with the experimental one.
- ²⁹L. Mantese and M. C. Downer (private communication).
- ³⁰N. Arzate, J. Mejía, B.S. Mendoza, and R. Del Sole, *Appl. Phys. B: Lasers Opt.* **68**, 629 (1999).
- ³¹S. Goedecker, *Comput. Phys. Commun.* **76**, 294 (1993); S. Goedecker, *SIAM J. Sci. Comput. (USA)* **18**, 1605 (1997).
- ³²N. Arzate and Bernardo S. Mendoza, *Phys. Rev. B* **63**, 125 303 (2001).